Heliyon 10 (2024) e34438

Contents lists available at ScienceDirect

Heliyon

journal homepage: www.cell.com/heliyon

Research article

Single-cell analysis revealed that MTIF2 could promote hepatocellular carcinoma progression through modulating the ROS pathway

Yu Wang [a,1], Jingqiu Zhang [b,1], Yu Yang [c], Jinhao Chen [c], Fengwu Tan [c], Jinfang Zheng [c,*]

[a] *Medical and Healthcare Center, Hainan General Hospital, Hainan Affiliated Hospital of Hainan Medical University, Haikou, 570102, China*
[b] *Department of Dermatology, Wuhan No. 1 Hospital, Tongji Medical College, Huazhong University of Science and Technology, Wuhan, 430022, China*
[c] *Department of Hepatobiliary and Pancreatic Surgery, Hainan General Hospital, Hainan Affiliated Hospital of Hainan Medical University, Haikou, 570102, China*

ARTICLE INFO

Keywords:
Hepatocellular carcinoma
MTIF2
Single-cell
SOD2
ROS pathway

ABSTRACT

Aims: To analyze the expression of mitochondrial translational initiation factor 2 (MTIF2) and the biological functions of the gene in hepatocellular carcinoma (HCC).
Background: The treatment of HCC treatment and its prognostic prediction are limited by a lack of comprehensive understanding of the molecular mechanisms in HCC. **OBJECTIVE**: To determine the cells expressing MTIF2 in HCC and the function of the MTIF2+ cell subpopulation.
Methods: Gene expression analysis on TIMER 2.0, UALCAN, and GEPIA databases was performed to measure the expression of MTIF2 in HCC tissues. Cell clustering subgroups and annotation were conducted based on the single-cell sequencing data of HCC and paracancerous tissues in the Gene Expression Omnibus (GEO) database. MTIF2 expression in different cell types was analyzed. Further, biological pathways potentially regulated by MTIF2 in each cell type were identified. In addition, protein-protein interaction (PPI) networks of MTIF2 with genes in its regulated biological pathways were developed. The cell function assay was performed to verify the effects of superoxide dismutase-2 (SOD2) and MTIF2 on HCC cells. Finally, we screened virtual drugs targeting MTIF2 and SOD2 employing database screening, molecular docking and molecular dynamics.
Results: MTIF2 showed a remarkably high expression in HCC tissues. We identified a total of 10 cell types between HCC tissues and paracancerous tissues. MTIF2 expression was upregulated in epithelial cells, macrophages, and hepatocytes. More importantly, high-expressed MTIF2 in HCC tissues was mainly derived from epithelial cells and hepatocytes, in which the reactive oxygen species (ROS) pathway was significantly positively correlated with MTIF2. In the PPI network, there was a unique interaction pair between SOD2 and MTIF2 in the ROS pathway. Cell function experiments showed that overexpression of MTIF2 enhanced the proliferative and invasive capacities of HCC, which could synergize with SOD2 to co-promote the development of HCC. Finally, molecular dynamics simulations showed that DB00183 maintained a high structural stability with MTIF2 and SOD2 proteins during the simulation process.

* Corresponding author.
E-mail address: zhengjf71@sina.com (J. Zheng).
[1] Equal Contribution: These authors contributed equally in this study.

https://doi.org/10.1016/j.heliyon.2024.e34438
Received 18 April 2024; Received in revised form 9 July 2024; Accepted 9 July 2024
Available online 10 July 2024

Conclusion: Our study confirmed that the high-expressed MTIF2 in HCC tissues was derived from epithelial cells and hepatocytes. MTIF2 might act on SOD2 to regulate the ROS pathway, thereby affective the progression of HCC.

1. Introduction

HCC is the most frequently diagnosed primary liver tumor, but the molecular mechanisms underlying HCC development are not comprehensively understood [1,2]. Previous studies showed that most HCC patients would develop acquired resistance shortly after their initial use of targeted drugs [3–6]. The interactions between HCC cells and the tumor microenvironment (TME) could be a promising directions for investigating the molecular mechanisms underlying HCC development and metastasis [7,8]. The TME consists of tumor cells, immune cells, stromal cells, and associated extracellular matrix molecules that significantly influence the development of the malignant phenotype of cancer cells through specific interactions [9]. It has been shown that the disruption of tight intercellular junctions between epithelial cells in HCC leads to a loss of primitive polarity, order, and coherence, which in turn promotes an epithelial-to-mesenchymal (ETM) transition, enabling epithelial cells to exhibit mesenchymal cellular characteristics and develop migratory capacity [10]. Furthermore, growing evidence indicated that natural killer (NK) cells are influenced by liver diseases and liver cancers, such as HCC. Impaired function of NK cells will hinder their ability to eliminate virus-infected or tumor cells [11]. However, the molecular drivers of HCC carcinogenesis are currently unknown, and we face a lack of specific biomarkers for early diagnosis or as potential therapeutic targets for HCC treatment.

Single-cell transcriptome sequencing (scRNA-seq) analyzes gene expression at single-cell level by non-targeted quantification of transcripts in a single cell, allowing for in-depth investigation of cell types, cell functions, cell subpopulations and heterogeneity. At present, scRNA-seq is also commonly used for identifying new cell types, confirming rare cell populations, and constructing atlases of cell states and phylogenies [12–14]. In the field of oncology, scRNA-seq technology has been widely employed in studying tumor heterogeneity [15,16], tumor metastasis [17,18], tumor microenvironment [19–21], and antitumor drug discovery and development [22,23]. ScRNA-seq could help discover new biomarkers for cancers. For example, by integrating scRNA-seq and conventional RNA-seq data, Jiang et al. constructed a prognostic model for patients with lung adenocarcinoma (LUAD) and identified different cell subtypes to explore their different prognostic and immune characteristics [24]. Additionally, other researchers performed single-cell analysis to provide a comprehensive understanding of the recurrent HCC ecosystem and novel insights into the immune evasion mechanisms associated with tumor recurrence [25].

This study identified specific hepatocyte and epithelial cell types based on the RNA-seq data of HCC samples and the biological pathways and potential connections between the two types of cells were explored through multiple data analyses. The aim of this study was to elucidate different cell types in HCC and to provide new insights for HCC prognosis and treatment.

2. Materials and methods

2.1. Analysis of MTIF2 expression level

Differential expression of MTIF2 [26] in pan-cancer was analyzed between tumor and normal (Gene_DE) module of the TIMER 2.0 database (http://timer.cistrome.org/). The Gene_DE module was used to study the differential expression of genes of interest between the tumor and adjacent normal tissue in all TCGA tumors [27,28]. HCC tissues and normal tissues in the GEPIA database (http://gepia.cancer-pku.cn/) [29] and UALCAN database (https://ualcan.path.uab.edu/index.html) [30,31] were explored to determine the expression level of MTIF2. Notably, in the GEPIA software, we used the module "Expression DIY" and visualized the results in a box plot. Subsequently, we entered the name of the gene MTIF2 in the UALCAN online analysis software and selected the TCGA-LIHC dataset to analyze the expression level of MTIF2 in LIHC.

2.2. Single-cell data analysis

To analyze the differences in cell profiles between HCC and normal liver tissues, a single-cell cohort containing five HCC samples and five paracancerous tissues, GSE242889 was collected from the GEO database (https://www.ncbi.nlm.nih.gov/geo/). The data format of GSE242889 was count matrix. The Seurat package [32] was utilized for data reading and processing. Cells with mitochondrial gene ratio <25 % and gene counts between 200 and 5000 were retained. Data normalization was performed by the built-in SCTransform function in the Seurat package, followed by performing principal component analysis (PCA). Subsequently, the harmony package [33] was used to eliminate the batch effect between the 10 samples. The first 30 principal components were selected for Uniform Manifold Approximation and Projection (UMAP) dimensionality reduction analysis. Cells were clustered and analyzed applying the FindNeighbors and FindClusters functions in the Seurat package at the resolution $= 0.1$. The marker genes of the cells were extracted from the CellMarker database (http://xteam.xbio.top/CellMarker/) [34], and clusters of cells were annotated according to their expression levels to determine the cell type.

2.3. Hallmark pathway activity score

The h.all.v2023.1.Hs.symbols.gmt file was loaded from the Molecular Signatures Database (MsigDB, https://www.gsea-msigdb.org/gsea/msigdb), which contained 50 hallmark pathways and corresponding gene sets. The activity scores of the hallmark pathways in different cell types were calculated using the AUCell package [35] and evaluated in terms of Area under the Curve (AUC) values. The correlation between MTIF2 and ROS pathway activity was assessed using the spearman correlation analysis.

2.4. Protein-protein interaction (PPI) networks

Gene sets containing MTIF2 in the ROS pathway were extracted and uploaded to the STRING database (https://cn.string-db.org/) [36] and PPI networks were developed. The threshold was set to medium confidence (0.400) to obtain the protein interaction pairs, and finally the PPI networks were visualized using the cytoscape software [37].

2.5. Cell culture and transfection

Cultures of THLE-2 cells (CRL-2706, ATCC, Rockville, MD, USA) and Huh7 cells (Institute of Basic Medical Sciences CAMS 3111C0001CCC000679) were conducted in Dulbecco's Modified Eagle medium (DMEM) containing 10 % fetal bovine serum (FBS) at 37 °C. Overexpression experiments of MTIF2 and SOD2 were performed by transfecting the cells with commercially available overexpression vectors for MTIF2 and SOD2, respectively, and negative controls (NC) were transfected with empty vectors. Knockdown experiments of MTIF2 were performed by transfecting the cells with small interfering RNAs (siRNAs) specific for MTIF2 mRNAs, and the controls were transfected with non-specific siRNAs (si-NC).

2.6. Quantitative real-time PCR

Total cellular RNA was extracted using Trizol reagent (Invitrogen), after which cDNA was obtained using reverse transcription with a cDNA synthesis kit (Bio-Rad, 1708890). MRNA for MTIF2 and SOD2 was analyzed by quantitative PCR using SYBR Green real-time PCR kit (Qiagen, Valencia, CA) and specific primers. Relative expression level was calculated using the $2^{-\Delta\Delta Ct}$ method [38] with GAPDH as an internal reference. The primer sequences were as follows: MTIF2 forward sequence 5′-3': GGAATGACTATTGAGGAACTGGC and reverse sequence 5′-3': CCTGCCTTCGTTATCACTTCTTT; SOD2 forward sequence 5′-3': CTGGACAAACCTCAGCCCTAAC and reverse sequence 5′-3': AACCTGAGCCTTGGACACCAAC.

2.7. Transwell assay

The upper chamber of the Transwell was pre-coated with Matrigel (Corning, 356231) to simulate the extracellular matrix. A suspension of treated cells was added to the upper chamber, while the lower chamber was supplemented with medium containing 10 % FBS as a chemotaxis agent. After cell incubation for 24 h (h), non-migrating cells in the upper chamber were removed, where cells invading the filter membrane were fixed and stained and then counted under a light microscope (Thermo Fisher Scientific, MA, USA).

2.8. Database preparation and molecular docking

This study utilized a database of 2614 chemical small molecules approved by the Food and Drug Administration (FDA) for virtual screening. All molecules were subjected to 3D structure transformation before docking using the LigPrep module of the Schrödinger software package. The energy of all the molecules were minimized using the OPLS4 force field, and their protonation state was predicted using the Epik method.

Next, based on the "Protein Preparation Wizard" module in the Maestro 13.0 software package for the protein preparation, the MTIF2 and SOD2 proteins with PDB IDs of 6GAZ and 5T30, respectively, were obtained from the Protein Data Bank (PDB) database. The proteins were processed with removal of water molecules, addition of missing hydrogen atoms, and repair of missing side chains. Subsequently, the amino acids were subjected to protonation state prediction at PH = 7.2, and energy minimization of the entire structure was performed using the OPLS4 force field.

Docking boxes were used to limit the spatial extent to search small molecules and are often used to wrap active pockets for docking [39]. The docking box files of the pockets were generated using the "Receptor Grid Generation" module in the Schrödinger 2021-4 software, and the binding site of the prepared proteins was predicted using the "sitemap" module. The top-ranked pockets were considered as the potentially active pockets at the centers of the boxes and further calculated to generate a grid file with a volume of 25*25*25 Å3. Finally, the structure-based virtual screening was performed using the "Glide" module. In this process, SP precision was used for docking, and the molecules obtained by docking were mapped and analyzed based on the scoring of the molecules of the two proteins showing a high binding affinity.

2.9. Statistical analysis

We used the Wilcoxon test to compare the difference between the two sets of continuous variables and the spearman correlation to measure the correlation between the two sets of continuous variables. $P < 0.01$ was considered statistically significant. All

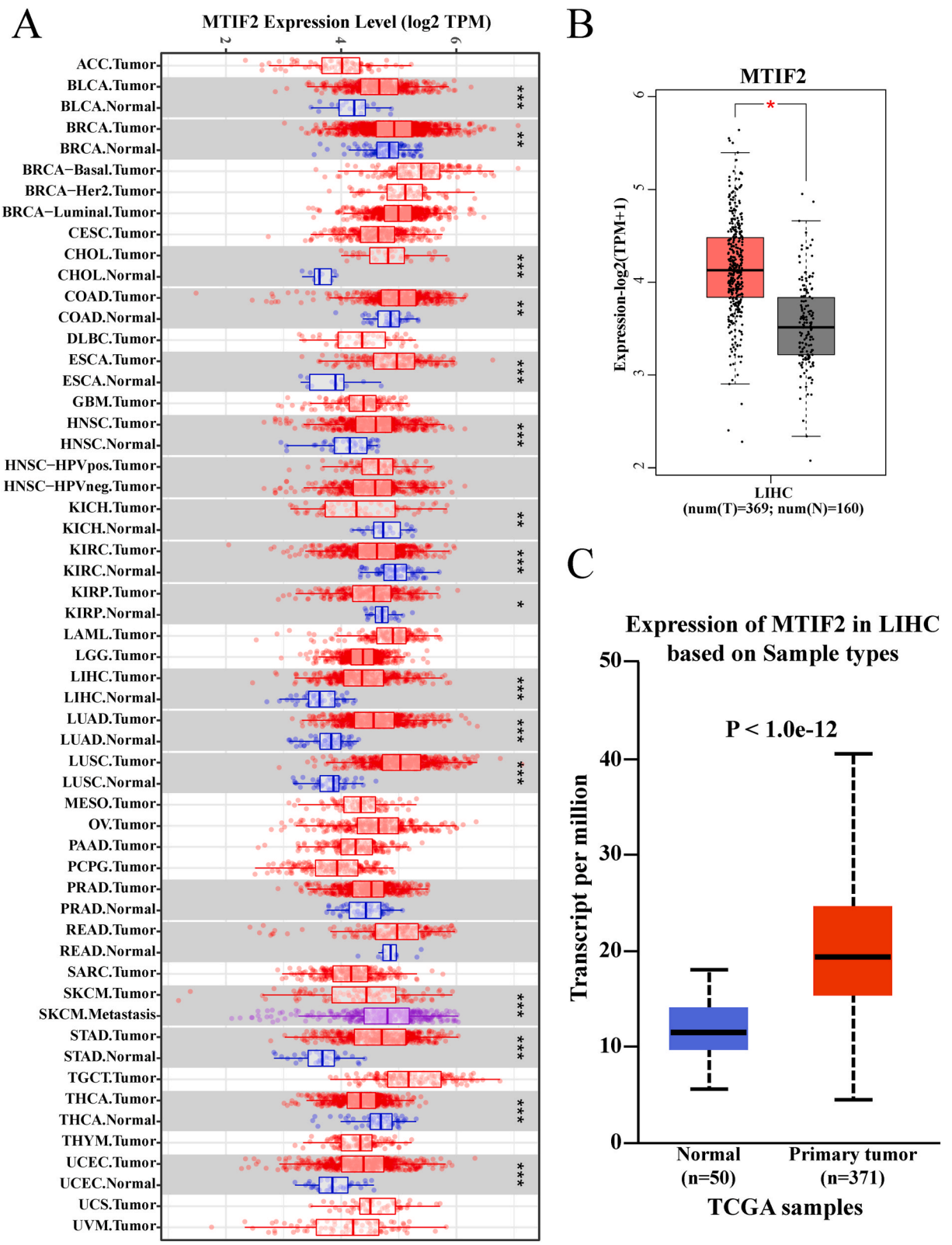

Fig. 1. MTIF2 expression was upregulated in HCC tissues. A: MTIF2 expression level in pan-cancer in TIMER 2.0 database.B: Expression level of MTIF2 in tumor tissues and normal tissues in GEPIA database.C: Expression levels of MTIF2 in tumor tissues and normal tissues in the UALCAN database.

computational procedures were completed using R language (version 3.6.0).

3. Results

3.1. MTIF2 expression was upregulated in HCC tissues

First, we measured the expression of MTIF2 in pan-cancer in the TIMER 2.0 database. The results showed that MTIF2 expression was upregulated in HCC tissues (Fig. 1A). In the GEPIA and UALCAN databases, we similarly examined the expression levels of MTIF2 in HCC tissues and normal tissues, and found that MTIF2 expression levels were abnormally upregulated in HCC tissues (Fig. 1B–C).

3.2. MTIF2 expression was upregulated in epithelial cells and hepatocytes

To further explore the expression levels of MTIF2 in different cell types, single-cell data derived from 5 HCC tissues and paracancerous tissues from the GSE242889 cohort were analyzed. Based on Seurat package processing and marker genes annotation,

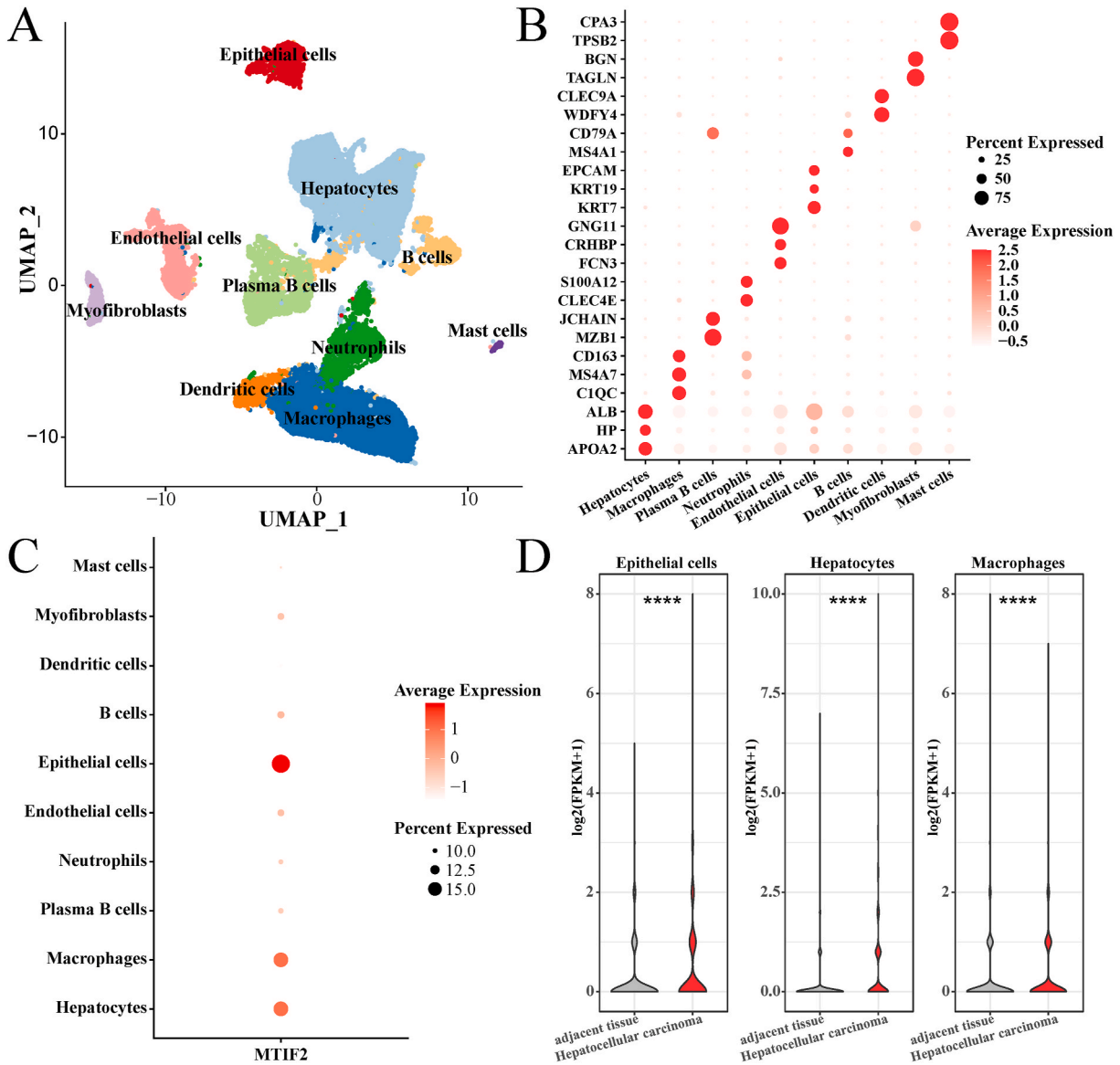

Fig. 2. MTIF2 expression was upregulated in Epithelial cells and Hepatocytes. A: 10 cell types identified in the GSE242889 cohort. B: Bubble plots of expression data of marker genes in 10 expression levels.C: MTIF2 expression levels in 10 cell types.D: MTIF2 expression levels in epithelial cells, macrophages, and hepatocytes in tumor tissues and paracancerous tissues.

we identified a total of 10 cell types, namely, epithelial cells, hepatocytes, B cells, endothelial cells, plasma b cells, myofibroblasts, neutrophils, mast cells, dendritic cells, and macrophages (Fig. 2A). The upregulated marker genes in the 10 cell types were shown in Fig. 2B. The expression of ALB, HP, and APOA2 was upregulated in hepatocytes, C1QC, MS4A7, CD163 were upregulated in macrophages, and EPCAM, KRT19, KRT7 were upregulated in epithelial cells. Next, the expression levels of MTIF2 in the 10 cell types were detected, and we found that it was upregulated in epithelial cells, macrophages, and hepatocytes (Fig. 2C). Interestingly, we extracted the expression matrix of the three types of cells in HCC tissues and para-cancerous tissues. It was found that MTIF2 was high-expressed in epithelial cells, hepatocytes of HCC origin, and macrophages of para-carcinoma tissue origin (Fig. 2D). These results suggested that the upregulation of MTIF2 could regulate epithelial and hepatocyte functions during HCC development.

3.3. Biological pathways regulated by MTIF2 in epithelial cells

Fifty hallmark pathways from the MsigDB database were collected, and we calculated their activity scores in epithelial cells using the AUCell package and performed a spearman correlation analysis between these pathways and MTIF2 expression level (Fig. 3A). It was found that upregulation of MTIF2 could activate adipogenesis, reactive oxygen species (ROS) pathway, oxidative phosphorylation,

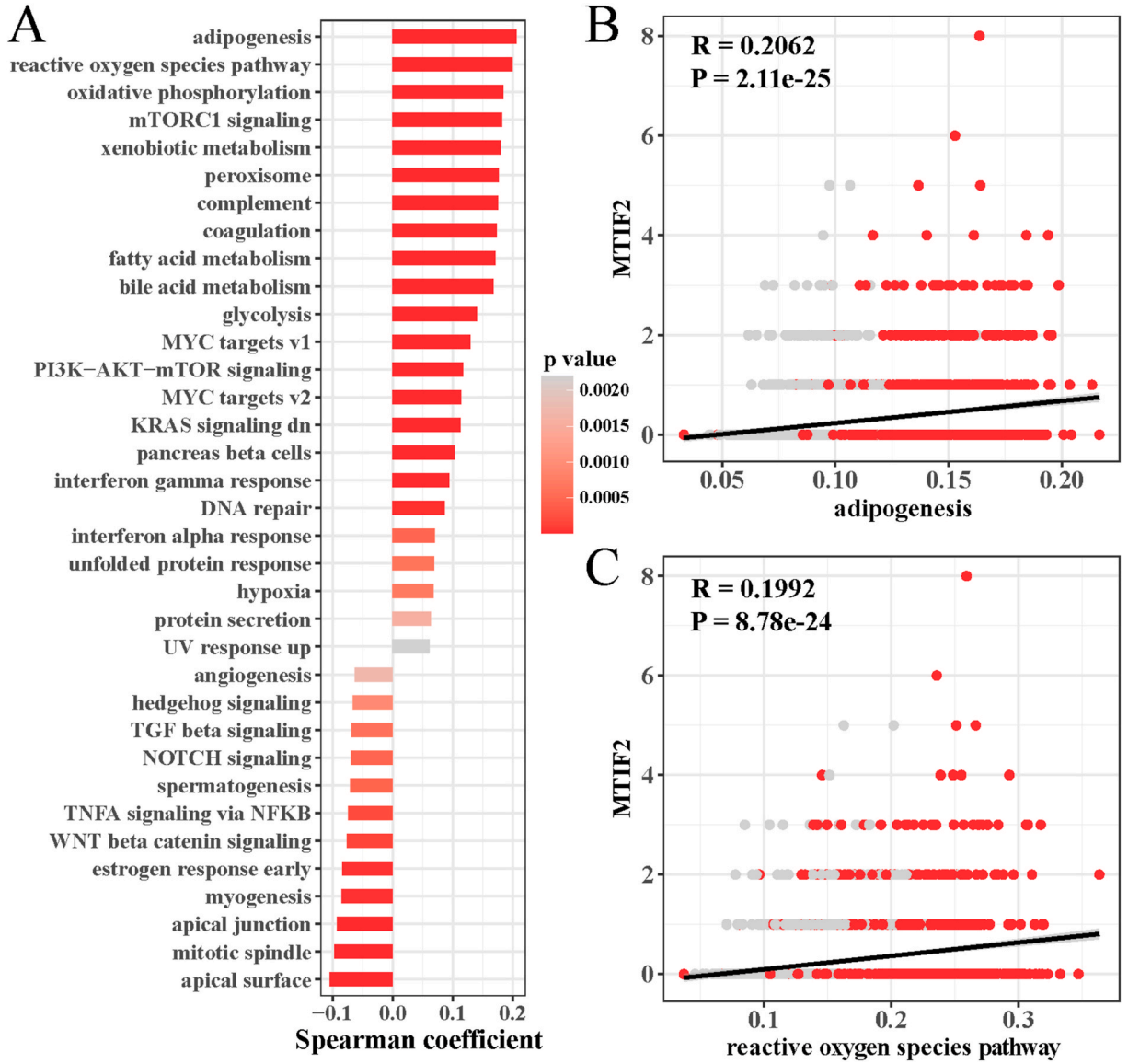

Fig. 3. Biological pathways regulated by MTIF2 in Epithelial cells. A: The spearman correlation of MTIF2 with hallmark pathway activity in Epithelial cells. B: Scatter plot of the spearman correlation between MTIF2 and adipogenesis activity.C: Scatter plot of spearman correlation between MTIF2 and ROS pathway activity.

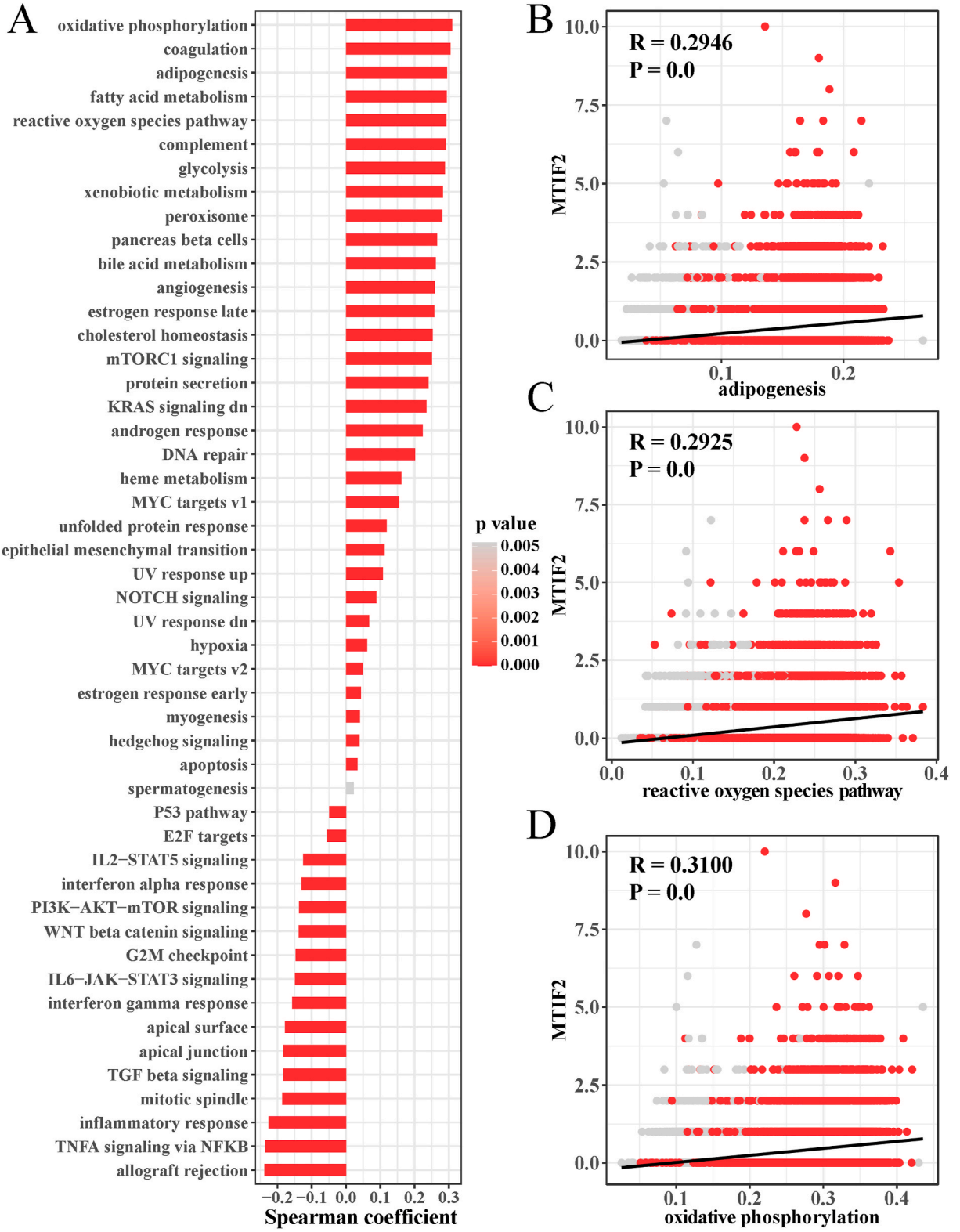

Fig. 4. Biological pathways regulated by MTIF2 in Hepatocytes. A: The spearman correlation of MTIF2 with hallmark pathway activity in Hepatocytes. B: Scatter plot of the spearman correlation between MTIF2 and adipogenesis activity.C: Scatter plot of spearman correlation between MTIF2 and ROS pathway activity.D: Scatter plot of spearman correlation between MTIF2 and oxidative phosphorylation activity.

and mTORC1 signaling, and xenobiotic metabolism in epithelial cells. MTIF2 showed a significant positive correlation with adipogenesis (R = 0.2062, P = 2.11e-25) (Fig. 3B) and ROS pathway (R = 0.1992, P = 8.78e-24) (Fig. 3C). In addition, we also found a significant positive correlation between MTIF2 and several ROS pathway-related genes in epithelial cells, including MGST1, FTL, GPX3, and SOD1 (P < 0.01) (Fig. S1A).

3.4. Biological pathways regulated by MTIF2 in hepatocytes

Similarly, we evaluated the hallmark pathways potentially regulated by MTIF2 in hepatocytes. Upregulation of MTIF2 expression has the potential to activate oxidative phosphorylation, coagulation, adipogenesis, fatty acid metabolism, and ROS pathway in hepatocytes (Fig. 4A). MTIF2 expression levels were correlated with adipogenesis (R = 0.2946, P = 0.0) (Fig. 4B), ROS pathway (R = 0.2925, P = 0.0) (Fig. 4C), oxidative phosphorylation (R = 0.3100, P = 0.0) (Fig. 4D). In particular, in hepatocytes, MTIF2 was significantly positively correlated with multiple ROS pathway-related genes, such as MGST1, TXN, PRDX1, and SOD1 (P < 0.01) (Fig. S1B).

3.5. PPI network of MTIF2 and genes related to the ROS pathway

Based on the results of previous studies, we found that MTIF2 showed a significant positive correlation with the ROS pathway in both hepatocytes and epithelial cells. We extracted the genes in the ROS pathway and uploaded them together with MTIF2 to the

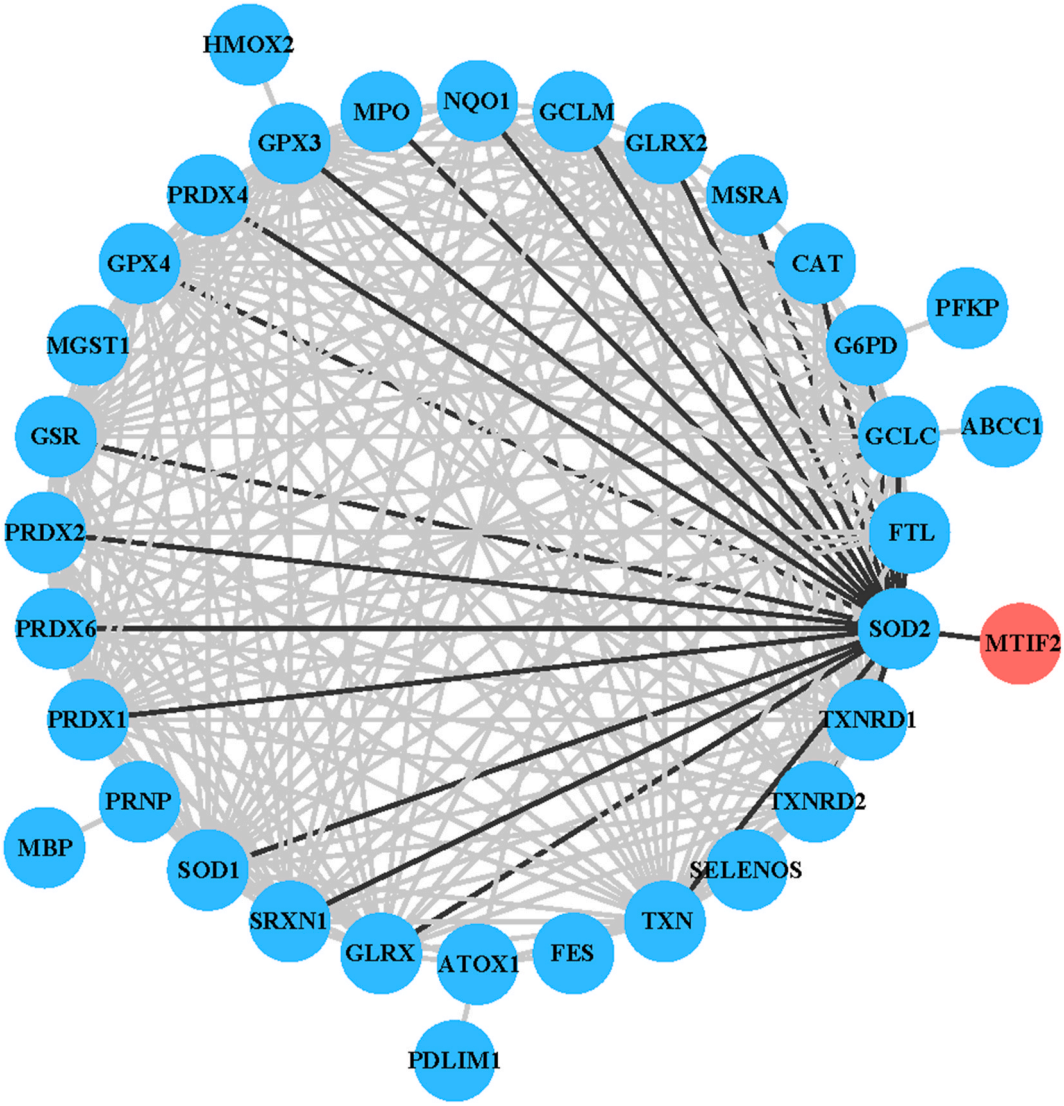

Fig. 5. PPI network of MTIF2 with genes within the ROS pathway.

STRING database to develop a PPI network. It was found that MTIF2 only interacted with SOD2, a gene that interacted with multiple proteins in the ROS pathway, such as GPX3, MSRA, MPO, and PRDX1. This indicated that MTIF2 may be involved in the interaction with SOD2 in the regulation of the ROS pathway (Fig. 5).

3.6. The expression of MTIF2 and SOD2 and functional analysis in HCC cells

To further validate the potential effects of MTIF2 and SOD2 on the pathogenesis of HCC, we first confirmed by qRT-PCR analysis that the mRNA expression MTIF2 and SOD2 was significantly upregulated in HCC cells compared with normal controls (Fig. 6A–B). In addition, as shown in Fig. 6C–D, cell invasion was enhanced under the condition of overexpression of MTIF2 (oe-MTIF2). When both MTIF2 and SOD2 were overexpressed, the invasive ability of the cells was promoted. After MTIF2 knockdown (si-MTIF2), the invasive ability of the cells was significantly reduced. These results indicated that overexpression of MTIF2 could elevate the proliferation and invasion ability of HCC, while overexpression of SOD2 can potentially synergize with MTIF2 to jointly promote the development of HCC.

3.7. Drug virtual screening analysis

MTIF2 and SOD2 proteins were docked using FDA-approved small molecule chemotaxis database, and we calculated docking scores for the top 100 molecules of these two proteins (Tables S1–2). It was observed that DB00183 had a high binding affinity to both MTIF2 and SOD2 both of −7.016 kcal/mol and −7.462 kcal/mol, respectively, indicating that the DB00183 molecule may be a dual-targeting drug simultaneously acting on MTIF2 and SOD2. The structural formula of the DB00183 molecule was shown in Fig. 7A. Subsequently, analysis on the binding mode of DB00183 and MTIF2 protein showed that the small molecule bound in the upper cavity of the protein and hydrogen bonds with GLU-209, THR-194, THR-214, THR-195, LYS-289, ASP-263, and ASP-190 on the protein. In addition, hydrophobic interactions with ILE-213 and LEU-326 were observed (Fig. 7B). These interactions were the basis for the stable binding between DB00183 and MTIF2 protein. As shown in Fig. 7C, based on the binding pattern of DB00183 and SOD2 protein, we

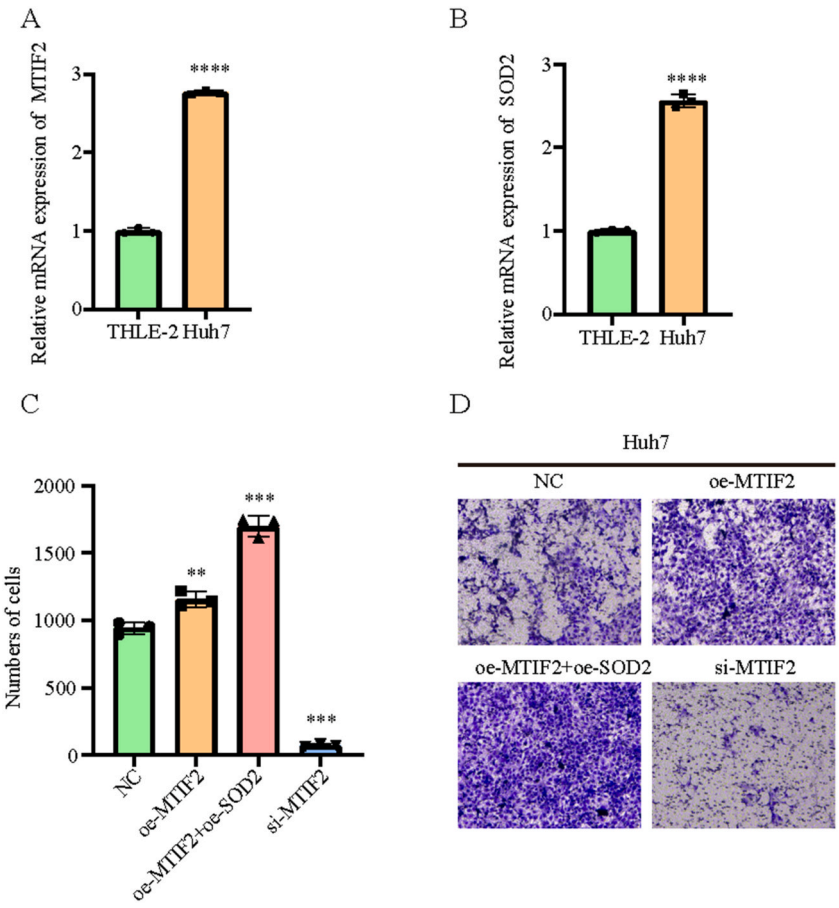

Fig. 6. Effects of MTIF2 and SOD2 on HCC cells. A: MTIF2 mRNA expression levels in THLE-2 and Huh7 Cells. B: SOD2 expression profiles in normal and HCC cells.C–D: Invasive potential of Huh7 cells under different MTIF2 and SOD2 expressions.

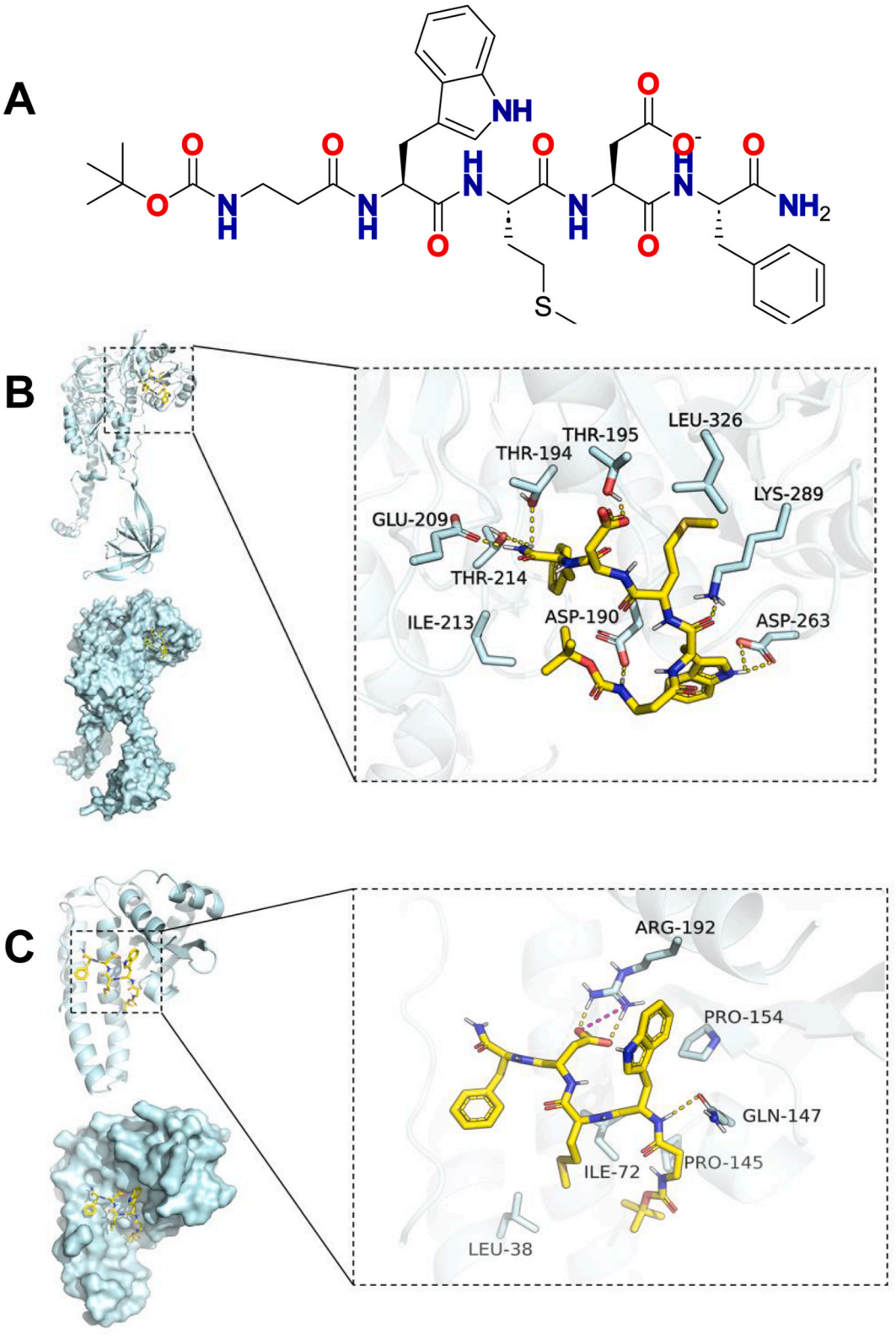

(caption on next page)

Fig. 7. Binding mode of DB00183 to MTIF2 and SOD2 proteins. A: Structural formula of the molecule DB00183. B: Diagram of the binding pattern of DB00183 and MTIF2 proteins. The left figure shows the overall view and the right figure shows the partial view. Yellow stick indicates DB00183, cyan indicates MTIF2 protein, and yellow dashed line indicates hydrogen bonding interaction.C: Diagram of the binding pattern of DB00183 and SOD2 protein. The left panel shows the overall view and the right panel shows the partial view. Yellow stick indicates DB00183 and cyan indicates SOD2 protein. Yellow dashed lines indicate hydrogen bonding interactions, and red dashed lines indicate salt-bridging interactions.

found that the small molecule bound in the upper cavity of the protein, hydrogen-bonding with ARG-192 and GLN-147 on the protein, and salt-bridging with ARG-192. In addition, hydrophobic interactions with LEU-38, ILE-72, PRO-145, and PRO-154 were observed. These interactions supported a stable binding between DB00183 and SOD2 proteins.

4. Discussion

At present, we face a lack of effective strategy to prevent the recurrence of HCC and improve the prognosis of the cancer [40,41]. Previous studies showed that MTIF2 is the main factor leading to a poor efficacy of 5-FU in treating HCC. Though chemotherapeutic agents promote immunogenic cell functional activity, MTIF2 can resist cancer treatment by mediating immunogenic cell death through the inhibition of MTIF2 expression in HCC cells [42]. Hall et al. showed that altered lipid profiles were responsible for the proliferation of hepatocytes in HCC [43]. MTIF2 is inextricably linked to mitochondrial function, and Lee et al. indicated that inhibition of MTIF2 expression significantly downregulates the level of oxidative metabolism in cells [44]. The current data demonstrated a high expression of MTIF2 in epithelial cells and hepatocytes in HCC tissues. The proliferation of hepatocytes might be caused by a high expression of MTIF2 in the cells. Previous evidence demonstrated that epithelial cell adhesion molecules are a factor causing HCC cells resistant to 5-Fluorouracil (5-FU) [45]. MTIF2 could mediate 5-FU resistance in HCC [42]. The potential link between MTIF2 and epithelial cells remained to be further explored.

Accumulating evidence showed that ROS is an important factor in the development and treatment of cancer [46]. A high level of ROS concentration could trigger uncontrolled cell proliferation [47]. The ROS pathway is a potent tumor suppressor, and some chemotherapeutic drugs work to produce ROS to induce autophagy in tumor cells [48]. Our study identified the ROS pathway as a significantly activated biological pathway in hepatocyte and epithelial cells. Several studies have shown that inhibition of ROS pathway activity is the key in the successful treatment of HCC. It was found that in HCC, activation of the ROS pathway substantially activates hepatocytes to undergo EMT and migration [49]. The results of Vishnoi et al. indicated that enhanced mitochondrial damage and mitochondrial ROS production in HCC tissues could attenuate sorafenib resistance, and that enhanced drug sensitivity could improve the efficacy of chemotherapy in HCC [50]. Interestingly, MTIF2 is a critical initiator for fulfilling mitochondrial functions [51]. It has been shown that MTIF2 maintains oxidative properties of cardiomyocytes in obese mice [44]. Our study found that MTIF2 had a high expression in both epithelial cells and hepatocytes. However, the mechanism of action underlying the relationship between the expression level of MTIF2 and ROS and whether the expression of MTIF2 affected the cellular response to oxidative stress in HCC remained unclear. Therefore, we hypothesized that MTIF2 activated mitochondrial activity in HCC to mobilize the ROS pathway, which contributed to the progression of HCC.

Finally, we developed a PPI network based on genes in the MTIF2 and ROS pathway. In the network, only SOD2 and MTIF2 interacted with each other. SOD2 is a mitochondrial protein essential for tumor cell invasion and metastasis in cancer [52]. Under hypoxic conditions, SOD2 transcription will be activated to reduce mitochondrial ROS levels, resulting in breast cancer cell stemness and drug resistance [53]. In addition, the overexpression of SOD2 could significantly promote invasion and aggression of a variety of cancers *in vivo* and *in vitro* [54,55], which was similar to our findings. Ranganathan et al. observed that upregulated SOD2 in cancer cells was associated with an upregulation and heightened activity of MMPs, resulting in increased degradation of the matrix and the subsequent release of cytokines and growth factors to facilitate metastasis [56]. In particular, the high expression of SOD2 is associated with a significant survival advantage in HCC [57]. Inhibition of SOD2 expression in HCC promotes ROS accumulation and causes HCC cell metastasis [58]. Our study showed that SOD2 and MTIF2 interacted with each other, and we hypothesized that there might be a negative correlation between the two. MTIF2 inhibited SOD2 expression and ROS generation, leading to HCC progression.

However, this study still had certain limitations. First, our study relied heavily on the data from public databases, therefore future integration of multiple databases with more samples is required to improve the reliability of the current findings. In particular, MTIF2 expression analyzed with more relevant clinical data could serve as a prognostic marker for HCC. Moreover, wet experiments are needed to further validate the specific role of MTIF2 and its regulatory pathways in HCC. Although we revealed the binding relationship of DB00183 with MTIF2 and SOD2, we failed to explore its specific anticancer function in depth. Hence, future studies and experiments should be performed for systematic evaluation. Finally, this study mainly focused on the functions of MTIF2 and SOD2 and their roles in the ROS pathway without considering other potentially relevant genes and their regulatory networks. Hence, future studies are encouraged to systematically investigate the functions of relevant genes and their regulatory networks in HCC applying genome editing technology, transcriptomics and proteomics.

5. Conclusion

Overall, our study confirmed that the high expression of MTIF2 in HCC tissues were derived from hepatocyte and epithelial cells, and that activated MTIF2 may exacerbate cancer progression by inhibiting the transcription of SOD2 to activate the ROS pathway in HCC. Importantly, molecular dynamics simulations showed that the interaction of DB00183 with both MTIF2 and SOD2 protein had a

high structural stability. Our study explained the potential novel mechanism of MTIF2 in HCC applying bioinformatics, providing new insights into the diagnosis and treatment of HCC patients.

Funding

This study was funded by Natural Science Foundation of Hainan Province [821QN0980], Hainan Provincial Science and Technology Program (Hainan Clinical Research Center for Malignant Tumors of Digestive System) [LCYX202208] and Hainan Province Science and Technology Special Fund (Social Development Projects) [ZDYF2022SHFZ131].

Ethics approval and consent to participate

Not applicable.

Consent for publication

All authors have read and agreed to publish the article.

Availability of data and materials

The datasets generated and/or analyzed during the current study are available in the [GSE242889] repository, [https://www.ncbi.nlm.nih.gov/geo/query/acc.cgi?acc=GSE242889].

CRediT authorship contribution statement

Yu Wang: Writing – review & editing, Writing – original draft, Visualization, Supervision, Software, Project administration, Data curation, Conceptualization. **Jingqiu Zhang:** Visualization, Resources, Methodology, Investigation. **Yu Yang:** Visualization, Resources, Methodology, Conceptualization. **Jinhao Chen:** Visualization, Supervision, Resources, Methodology, Formal analysis. **Fengwu Tan:** Visualization, Software, Resources, Formal analysis, Data curation. **Jinfang Zheng:** Writing – review & editing, Validation, Supervision, Resources, Methodology, Funding acquisition.

Declaration of competing interest

The authors declare that they have no known competing financial interests or personal relationships that could have appeared to influence the work reported in this paper.

Acknowledgement

None.

Appendix A. Supplementary data

Supplementary data to this article can be found online at https://doi.org/10.1016/j.heliyon.2024.e34438.

Abbreviations

HCC	hepatocellular carcinoma
GEO	Gene Expression Omnibus
PPI	protein-protein interaction
ROS	reactive oxygen species
scRNA-seq	Single-cell transcriptome sequencing
PCA	principal component analysis
UMAP	Uniform Manifold Approximation and Projection
MsigDB	Molecular Signatures Database
AUC	Area Under the Curve

References

[1] C. Yang, et al., Evolving therapeutic landscape of advanced hepatocellular carcinoma, Nat. Rev. Gastroenterol. Hepatol. 20 (4) (2023) 203–222.

[2] X. Lin, et al., A novel immune-associated prognostic signature based on the immune cell infiltration analysis for hepatocellular carcinoma, Oncologie 26 (1) (2024) 91–103.
[3] R.L. Siegel, et al., Cancer statistics, 2023, CA Cancer J Clin 73 (1) (2023) 17–48.
[4] W. Tang, et al., The mechanisms of sorafenib resistance in hepatocellular carcinoma: theoretical basis and therapeutic aspects, Signal Transduct Target Ther 5 (1) (2020) 87.
[5] J. Khaled, et al., Drug resistance and endoplasmic reticulum stress in hepatocellular carcinoma, Cells 11 (4) (2022).
[6] L. Wei, et al., The emerging role of microRNAs and long noncoding RNAs in drug resistance of hepatocellular carcinoma, Mol. Cancer 18 (1) (2019) 147.
[7] A. Huang, et al., Targeted therapy for hepatocellular carcinoma, Signal Transduct Target Ther 5 (1) (2020) 146.
[8] S. Xia, et al., The microenvironmental and metabolic aspects of sorafenib resistance in hepatocellular carcinoma, EBioMedicine 51 (2020) 102610.
[9] B. Lv, et al., Immunotherapy: reshape the tumor immune microenvironment, Front. Immunol. 13 (2022) 844142.
[10] L. Yan, F. Xu, C.L. Dai, Relationship between epithelial-to-mesenchymal transition and the inflammatory microenvironment of hepatocellular carcinoma, J. Exp. Clin. Cancer Res. 37 (1) (2018) 203.
[11] P. Liu, L. Chen, H. Zhang, Natural killer cells in liver disease and hepatocellular carcinoma and the NK cell-based immunotherapy, J Immunol Res 2018 (2018) 1206737.
[12] G. Chen, B. Ning, T. Shi, Single-cell RNA-seq technologies and related computational data analysis, Front. Genet. 10 (2019) 317.
[13] S. Slovin, et al., Single-cell RNA sequencing analysis: a step-by-step overview, Methods Mol. Biol. 2284 (2021) 343–365.
[14] A. Zulibiya, et al., Single-cell RNA sequencing reveals potential for endothelial-to-mesenchymal transition in tetralogy of fallot, Congenit. Heart Dis. 18 (6) (2023) 611–625.
[15] E. Wei, et al., Integration of scRNA-seq and TCGA RNA-seq to analyze the heterogeneity of HPV+ and HPV- cervical cancer immune cells and establish molecular risk models, Front. Oncol. 12 (2022) 860900.
[16] H. Yang, Comprehensive analysis of the expression and clinical significance of a ferroptosis-related genome in ovarian serous cystadenocarcinoma: a study based on TCGA data, Oncologie 24 (4) (2022).
[17] K. Xu, et al., Integrative analyses of scRNA-seq and scATAC-seq reveal CXCL14 as a key regulator of lymph node metastasis in breast cancer, Hum. Mol. Genet. 30 (5) (2021) 370–380.
[18] D. Zhang, et al., Establishment of an ovarian cancer omentum metastasis-related prognostic model by integrated analysis of scRNA-seq and bulk RNA-seq, J. Ovarian Res. 15 (1) (2022) 123.
[19] Y. Katzenelenbogen, et al., Coupled scRNA-seq and intracellular protein activity reveal an immunosuppressive role of TREM2 in cancer, Cell 182 (4) (2020) 872–885 e19.
[20] Z. Tan, et al., Comprehensive analysis of scRNA-Seq and bulk RNA-Seq reveals dynamic changes in the tumor immune microenvironment of bladder cancer and establishes a prognostic model, J. Transl. Med. 21 (1) (2023) 223.
[21] Z. Fang, et al., Integration of scRNA-seq and bulk RNA-seq reveals molecular characterization of the immune microenvironment in acute pancreatitis, Biomolecules 13 (1) (2022).
[22] J. Chen, et al., Deep transfer learning of cancer drug responses by integrating bulk and single-cell RNA-seq data, Nat. Commun. 13 (1) (2022) 6494.
[23] S. Ding, X. Chen, K. Shen, Single-cell RNA sequencing in breast cancer: understanding tumor heterogeneity and paving roads to individualized therapy, Cancer Commun. 40 (8) (2020) 329–344.
[24] A. Jiang, et al., Integration of single-cell RNA sequencing and bulk RNA sequencing data to establish and validate a prognostic model for patients with lung adenocarcinoma, Front. Genet. 13 (2022) 833797.
[25] Y. Sun, et al., Single-cell landscape of the ecosystem in early-relapse hepatocellular carcinoma, Cell 184 (2) (2021) 404–421.e16.
[26] T. Li, et al., TIMER2.0 for analysis of tumor-infiltrating immune cells, Nucleic Acids Res. 48 (W1) (2020) W509–W514.
[27] T. Li, et al., TIMER: a web server for comprehensive analysis of tumor-infiltrating immune cells, Cancer Res. 77 (21) (2017) e108–e110.
[28] B. Li, et al., Comprehensive analyses of tumor immunity: implications for cancer immunotherapy, Genome Biol. 17 (1) (2016) 174.
[29] Z. Tang, et al., GEPIA: a web server for cancer and normal gene expression profiling and interactive analyses, Nucleic Acids Res. 45 (W1) (2017) W98–W102.
[30] D.S. Chandrashekar, et al., UALCAN: an update to the integrated cancer data analysis platform, Neoplasia 25 (2022) 18–27.
[31] D.S. Chandrashekar, et al., UALCAN: a portal for facilitating tumor subgroup gene expression and survival analyses, Neoplasia 19 (8) (2017) 649–658.
[32] T. Stuart, et al., Comprehensive integration of single-cell data, Cell 177 (7) (2019) 1888–1902 e21.
[33] I. Korsunsky, et al., Fast, sensitive and accurate integration of single-cell data with Harmony, Nat. Methods 16 (12) (2019) 1289–1296.
[34] X. Zhang, et al., CellMarker: a manually curated resource of cell markers in human and mouse, Nucleic Acids Res. 47 (D1) (2019) D721–D728.
[35] S. Aibar, et al., SCENIC: single-cell regulatory network inference and clustering, Nat. Methods 14 (11) (2017) 1083–1086.
[36] D. Szklarczyk, et al., The STRING database in 2021: customizable protein-protein networks, and functional characterization of user-uploaded gene/measurement sets, Nucleic Acids Res. 49 (D1) (2021) D605–D612.
[37] P. Shannon, et al., Cytoscape: a software environment for integrated models of biomolecular interaction networks, Genome Res. 13 (11) (2003) 2498–2504.
[38] K.J. Livak, T.D. Schmittgen, Analysis of relative gene expression data using real-time quantitative PCR and the 2(-Delta Delta C(T)) Method, Methods 25 (4) (2001) 402–408.
[39] N.M. Hassan, et al., Protein-ligand blind docking using QuickVina-W with inter-process spatio-temporal integration, Sci. Rep. 7 (1) (2017) 15451.
[40] R. Xu, et al., A novel prognostic target-gene signature and nomogram based on an integrated bioinformatics analysis in hepatocellular carcinoma, Biocell 46 (5) (2022) 1261–1288.
[41] M. Fang, et al., WGCNA and LASSO algorithm constructed an immune infiltration-related 5-gene signature and nomogram to improve prognosis prediction of hepatocellular carcinoma, Biocell 46 (2) (2022) 401–415.
[42] D. Xu, et al., MTIF2 impairs 5 fluorouracil-mediated immunogenic cell death in hepatocellular carcinoma in vivo: molecular mechanisms and therapeutic significance, Pharmacol. Res. 163 (2021) 105265.
[43] Z. Hall, et al., Lipid remodeling in hepatocyte proliferation and hepatocellular carcinoma, Hepatology 73 (3) (2021) 1028–1044.
[44] D.E. Lee, et al., Mitochondrial mRNA translation initiation contributes to oxidative metabolism in the myocardia of aged, obese mice, Exp. Gerontol. 121 (2019) 62–70.
[45] Y. Li, et al., Epithelial cell adhesion molecule in human hepatocellular carcinoma cell lines: a target of chemoresistence, BMC Cancer 16 (2016) 228.
[46] B.M. Sahoo, et al., Reactive oxygen species (ROS): key components in cancer therapies, Anti Cancer Agents Med. Chem. 22 (2) (2022) 215–222.
[47] E.C. Cheung, K.H. Vousden, The role of ROS in tumour development and progression, Nat. Rev. Cancer 22 (5) (2022) 280–297.
[48] K. Wang, Autophagy and apoptosis in liver injury, Cell Cycle 14 (11) (2015) 1631–1642.
[49] M. Jin, et al., MCUR1 facilitates epithelial-mesenchymal transition and metastasis via the mitochondrial calcium dependent ROS/Nrf2/Notch pathway in hepatocellular carcinoma, J. Exp. Clin. Cancer Res. 38 (1) (2019) 136.
[50] K. Vishnoi, et al., Ets1 mediates sorafenib resistance by regulating mitochondrial ROS pathway in hepatocellular carcinoma, Cell Death Dis. 13 (7) (2022) 581.
[51] Y. Itoh, et al., Mechanism of mitoribosomal small subunit biogenesis and preinitiation, Nature 606 (7914) (2022) 603–608.
[52] N. Alateyah, et al., SOD2, a potential transcriptional target underpinning CD44-promoted breast cancer progression, Molecules 27 (3) (2022).
[53] Y. Yan, et al., A novel HIF-2alpha targeted inhibitor suppresses hypoxia-induced breast cancer stemness via SOD2-mtROS-PDI/GPR78-UPR(ER) axis, Cell Death Differ. 29 (9) (2022) 1769–1789.
[54] I. Quirós, et al., Upregulation of manganese superoxide dismutase (SOD2) is a common pathway for neuroendocrine differentiation in prostate cancer cells, Int. J. Cancer 125 (7) (2009) 1497–1504.
[55] K.M. Connor, et al., Manganese superoxide dismutase enhances the invasive and migratory activity of tumor cells, Cancer Res. 67 (21) (2007) 10260–10267.

[56] A.C. Ranganathan, et al., Manganese superoxide dismutase signals matrix metalloproteinase expression via H2O2-dependent ERK1/2 activation, J. Biol. Chem. 276 (17) (2001) 14264–14270.
[57] R. Wang, et al., Reduced SOD2 expression is associated with mortality of hepatocellular carcinoma patients in a mutant p53-dependent manner, Aging (Albany NY) 8 (6) (2016) 1184–1200.
[58] T. Ren, et al., MCU-dependent mitochondrial Ca(2+) inhibits NAD(+)/SIRT3/SOD2 pathway to promote ROS production and metastasis of HCC cells, Oncogene 36 (42) (2017) 5897–5909.